ELEKTROTEHNIŠKI VESTNIK 86(4): 211-218, 2019
ORIGINAL SCIENTIFIC PAPER

Experimental Characterization of the High-Frequency Isolating Power Transformer

Mohamed Miloudi [1, 2], Houcine Miloudi [2], Abdelber Bendaoud [2], Mohammed Adnan Salhi [3], Ahmad N. Al-Omari [4]

[1]*Electrical Engineering Department, Ahmed Zabana University Center, Relizane, Algeria*
[2]*APELEC Laboratory of Djilali Liabes University, Sidi Bel Abbes, Algeria*
[3]*Physikalisch-Technische Bundesanstalt, Braunschweig, Germany*
[4]*Electronics Engineering Department, Yarmouk University, Irbid, Jordan*
[1]*E-mail: mohamed.miloudi@univ-sba.dz*

Abstract. The paper presents results of measurements, simulations and calculations of parasitic capacitances of a high-frequency (150 kHz to 30 MHz) double-winding transformer. Practical techniques to determine its stray capacitances as well as a method for transformer parameter determination are proposed. An equivalent-circuit method taking into account the lumped parameters of this component and EMC tests are presented. Results of analytical calculations are compared with the experimental ones obtained on the basis of the resonance effect. A good agreement is shown between the measured and simulated results. At the end, the presented procedures and safety measures are tested and validated.

Keywords: high-frequency, transformer, winding, stray capacitances, impedance measurements.

Karakterizacija visokofrekvenčnega dvonavitnega transformatorja

V prispevku predstavljamo teoretične izračune, rezultate simulacij in meritev parazitnih kapacitivnosti v visokofrekvenčnem (150 kHz to 30 MHz) dvonavitnem transformatorju. Opisani so pristopi za določitev stresanih kapacitivnosti in parametrov transformatorja. Predstavljeni so ekvivalentno vezje transformatorja in rezultati testa EMC. Teoretični izračuni so primerljivi z rezultati, pridobljenimi pri simulaciji. Opisani so testni merilni sistem in rezultati meritev.

1 INTRODUCTION

In isolated power-supply applications, the transformer parasitic capacitance can significantly affect the converter operation. Some of the adverse effects are distortion of the current waveform on the excitation side or a decrease in the overall converter efficiency. Subjected to high-voltage stresses, the inter-winding capacitance causes leakage currents and, consequently, EMI problems [1]. The simulation-based EMC analysis of transformers and virtualization of the system EMC tests are actively investigated by multiple research groups [1–5]. Taking EMI into account in the initial design stage can ensure designers to satisfy EMC at a low cost before realization [6]. Traditionally, electronic devices are characterized, modeled and analyzed in the frequency-domain. Power electronics are analyzed mainly with impedance parameters used to determine the number and placement of decoupling capacitors [7, 8]. Miniaturization, increasing complexity and speed of data transferring by modern electronic devices used in transformers cause big challenges for the implementation of electromagnetic compliance of digital blocks [9]. A high-frequency transformer is a critical block of the power conversion system [10, 11].

The transformer electric parameters, including those of a parasitic nature, do not only determine the correct operation of the transformer itself, but also affect the operation conditions of elements directly connected with the transformer windings, as well as the properties of the whole power electronic unit [12].

The transformer study is not a new topic [1–5], [13–17] and the corresponding studies have been conducted along the development of the power systems and power conversion technologies. This work focuses on the high-frequency transformer design for the high-frequency and high-power applications. A background description and review to help define this work and its novelty are presented. The proposed method to identify the capacitive behavior consists of placing oneself in simple situations where only two potentials are independent.
As soon as a certain component is characterized, the accuracy and frequency validity limit required for the model can be taken into account [18]. Thus, it is possible to progressively complete the equivalent scheme until the desired goal is achieved. New measurements and device characterization methods are needed [19].

Received 7 January 2019
Accepted 3 June 2019

Since a triple-measurement configuration can be used to identify the model, consistency checks are possible. Due to the inaccuracies mentioned above, the parameters significantly depend on the configurations used in the investigation [20]. Therefore, the inaccuracy of the final model is due to the investigation inconsistency.

In linear circuit characterization, voltages in vacuum short-circuit current gains, and trans-impedance measurements are often used. Using the Hewlett Packard HP4194A1B Impedance/Gain-Phase analyzer, the latter type of the measurements is investigated.

Indeed, when a measurement is made between two terminals different from those supplied, the impedance placed between them is never ideal, especially at high frequencies. At best, the infinite impedance is a weak capacitance and the impedance is a low inductance. However, the deviations caused by these parasitic impedances are very difficult to evaluate and compensate, whereas the open-short-load corrections provided for impedance measurements prove very effective provided the component is connected properly.

2 Model of a High-Frequency Transformer

The main objective of using the high-frequency transformer in the switching power supply is to step-up or step-down the input voltage and to isolate the output from the input of the circuit. When the operating frequency of a transformer is increased, it allows the transformer size to be smaller. However, the conducted EMI and its harmonics increase when the components work at their switching frequency [21]. Moreover, the magnetic components are widely used in power electronics at all levels of the energy conversion chain. This has motivated different research groups to investigate and focus on modelling these components and circuits [22-27].

In general, the circuit of a double-winding high-frequency transformer consists of two parts connected in parallel. One is magnetic and the other electrostatic. The magnetic part is represented by the inductance matrix and the electrostatic part by the capacitance matrix. Fig. 1 shows a double-winding transformer with magnetic and electrostatic part.

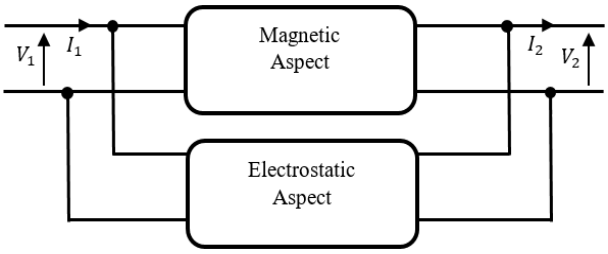

Figure 1. Magnetic and electrostatic aspect in the double-winding transformer.

2.1 Magnetic aspect

To describe the magnetic coupling of a transformer, the structure of the standard equivalent circuit of the transformer is used. The double-winding transformer is not considered as an ideal component but rather as a circuit element that performs a well-defined mathematical operation and is called a coupling element (Fig. 2). This structure combines a perfect transformer, a coupler, magnetizing inductance (L_p) and leakage inductance (L_s). To calculate L_p, it is assumed that the magnetic flux flows primarily in the magnetic core, which is true only for the infinite permeability cores. Fig. 2 is characterized by three values derived from the three independent elements of the associated inductance matrix. The characteristic quantities of this circuit are also derived from three measurements. If L_{02} is the inductance seen from the secondary, the primary is empty, if L_{01} is the inductance seen from the primary, the secondary is empty, and if L_{cc2} is the inductance seen from the secondary, the primary is short-circuited.

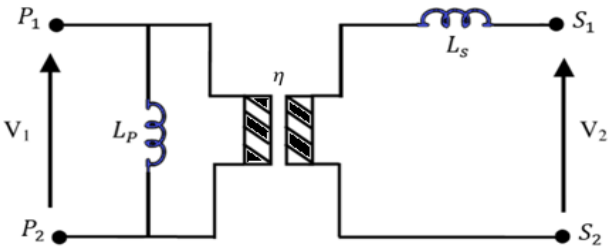

Figure 2. Transformer magnetic model.

Transformer ratio η is obtained from three inductance measurements:

$$L_P = L_{01} \tag{1}$$

$$L_s = L_{cc2} \tag{2}$$

$$\eta = \sqrt{\frac{L_{02} - L_s}{L_P}} \tag{3}$$

The module-phase representation makes it possible to precisely locate the resonance, but to identify the magnetizing inductance, the representation in L_p is more convenient (Fig. 3). The curve presented is noted while the secondary is floating. Here, a low-frequency value is taken (L_p = 88.34 μH).

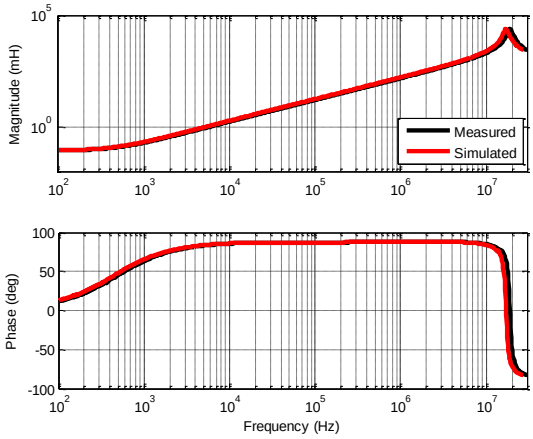

Figure 3. Measured and simulated magnetizing inductance.

Measuring the inductance of one winding when the other is short-circuited is more delicate. Indeed, at a low-frequency, when the magnetizing inductance is not completely shunted by resistance, it can contribute to the measurement.

Despite this inconvenience, a large variation in the leakage inductance as a function of the frequency is observed (Fig. 4). Its value is Ls = 202.9 μH (a low-frequency value).

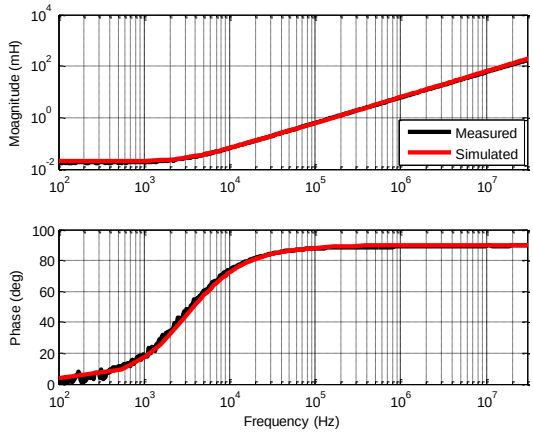

Figure 4. Measured and simulated leakage inductance.

2.2 Electrostatic aspect

A simplified electrostatic model of a double-winding transformer is characterized by three components distributed between the magnetic and electrostatic coupling. A simplified representation of a double-winding transformer is given in Fig. 5. These must be three capacitors between the four terminals of the coupler. The three magnetic constants are now known. It is magnetizing inductance L_p, leakage inductance L_S, and transformation ratio η. Capacitors C_2 and C_3 connected to terminal S_1 can be indifferently connected to one or the other side of the magnetizing inductance.

Finally, the simplified model of a double-winding transformer is characterized by, six constants. Three are magnetic and three electrostatic. The former are the magnetizing inductance L_p, leakage inductance L_S, and transformation ratio η, and the latter are C_1, C_2 and C_3.

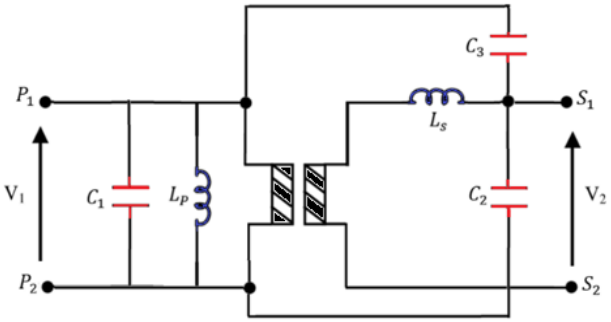

Figure 5. Simplified representation of a transformer.

In the isolating power transformer, there are inter-winding capacitances between each isolated winding. Therefore, C_1, C_2 and C_3 are the new components to calculate and implement in the model. Several measurements are made of the vacuum impedance seen from the transformer primary during the three measurements. The magnetizing inductance is in parallel of a different capacitance depending on the three desired capacitances.

The three measurements of the C_{mi} capacitance are sufficient to find the three parasitic capacitances (C_1, C_2 and C_3). The three measurements give the capacitance value. If can be easily obtained since the magnetizing inductance (L_p) is already known.

$$C_{mi} = \frac{1}{L_P.\omega_{ri}^2} \quad (4)$$

$$\omega_{ri} = 2.\pi.f_{ri} \quad (5)$$

The first step of the progressive method is to identify the inter-coil capacitance. In the case of a double-winding transformer, there is only one. For these measurements, the parallel representation is used, enabling a direct estimation of the capacitance. Fig. 6 shows a measurement of the transformer responses based on the test setup.

$$C_{m0} = C_2 + C_3 \quad (6)$$

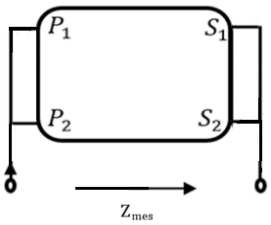

Figure 6. Configuration of the impedance measurement (C_{m0}).

Fig. 7 shows a slight increase in the capacitance as the frequency increases. The measured low-frequency value (C_{m0} = 300.2 pF) is taken. This variation in the capacitance is systematic. Moreover, none of our models can explains the step rise in its value at a high-

frequency since a system, with no free winding potential has no resonance.

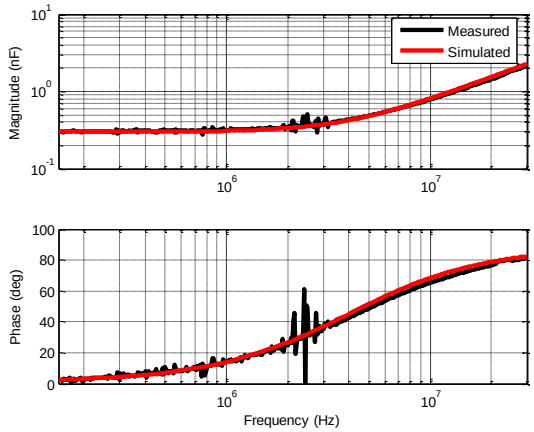

Figure 7. Measured and simulated impedance C_{m0}.

3 Measurement Setup and Experimental Results

The paper presents a comprehensive method of theoretical prediction as well as analytical expressions for theoretical prediction at different frequencies used for performance analysis during the design stage. EMI modeling is well covered in the literature using the time-domain and frequency-domain approaches [28]. To accurately determine EMI, the measurement setup is modeled according to the EMC standard recommendations [29].

Traditionally, EMI receivers perform measurements in the frequency-domain. They are heterodyne receivers that are tuned consecutively to different frequencies so as to cover the entire band with the requested resolution bandwidth [30].

EMC is a field dependent on experiences [31]. The measurements are performed in the frequency range from 150 kHz to 30 MHz compliably with the international EMC standard CISPR 16-1-1 [32]. The studied transformer primary and secondary voltage are 124V and 52V, respectively.

The vacuum impedance is pressured from the transformer primary (Fig. 8) by connecting the transformer primary to the impedance analyzer. The measurement is associated with capacitance C_{m1} given by:

$$C_{m1} = C_1 + C_2 \tag{7}$$

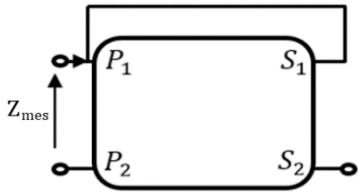

Figure 8. Configuration of impedance C_{m1} measurement.

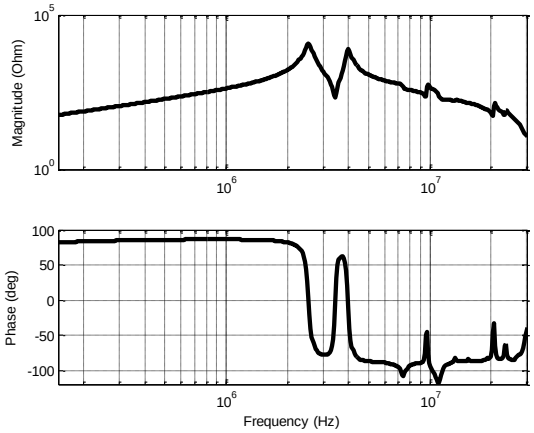

Figure 9. Impedance measurement associated with C_{m1}.

Fig. 9 shows the asymptotic Bode diagram associated with capacitance C_{m1} measurement. The first resonance frequency (peak of the impedance module) is f_{r1} = 2.538 MHz.

The second measurement (Fig. 10) of the vacuum impedance seen from the transformer primary side is associated with capacitance C_{m2} given by:

$$C_{m2} = C_1 + C_3 \tag{8}$$

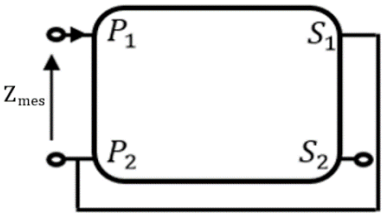

Figure 10. Configuration of the impedance C_{m2} measurement.

Fig. 11 shows the asymptotic Bode diagram associated with the capacitance C_{m2} measurement. The first resonance frequency is f_{r2} = 15.69 MHz.

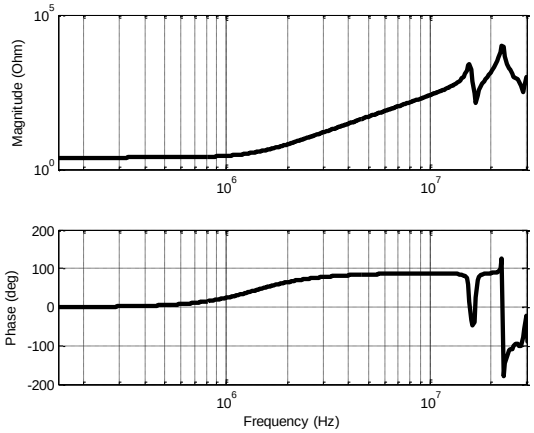

Figure 11. Impedance measurement associated with C_{m2}.

The last measurement (Fig. 12) of the vacuum impedance seen from the transformer primary is associated with capacitance C_{m3} given by:

$$C_{m3} = C_1 + \frac{C_2 C_3}{C_2 + C_3} \quad (9)$$

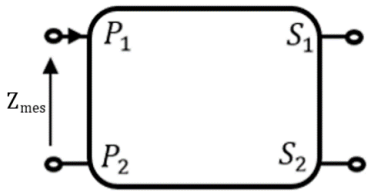

Figure 12. Configuration of impedance C_{m3} measurement.

Fig. 13 shows the asymptotic Bode diagram associated with the capacitance C_{m3} measurement. The first resonance frequency is f_{r3} = 3.056 MHz.

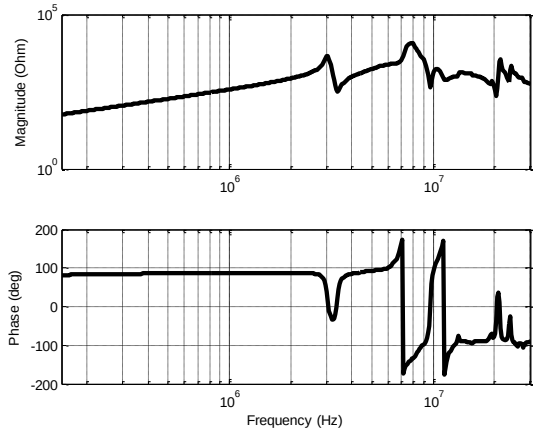

Figure 13. Impedance measurement associated with C_{m3}.

To enable a complete electrostatic characterization and implement a precise model covering higher frequencies, the leakage inductance is taken into account to determine the capacitances. The three potentials are independent and six capacitances are needed. Fig. 14 shows a complete representation of the transformer equivalent diagram based on its simplified representation.

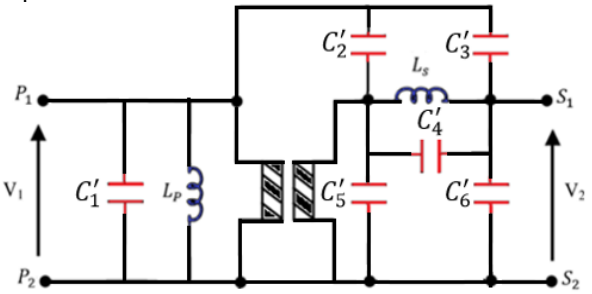

Figure 14. Complete equivalent diagram of a transformer.

This arrangement highlights the role of the leakage inductance. At a low-frequency, when the impedance is low, capacitances C_5' and C_6' are in parallel, and so are also C_2' and C_3'. To obtain simple equations, three complementary measures are taken to move from the partial model to a full model (Fig. 15). The measurements (Figs. 15, 17 and 19) show that the first resonance frequency is much lower than the series resonance indicating that the windings are very well coupled.

Capacitance C_{m4} given by:

$$C_{m4} = C_2' + C_4' + C_6' \quad (10)$$

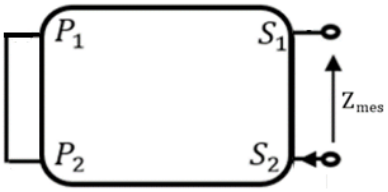

Figure 15. Configuration of the impedance C_{m4} measurement.

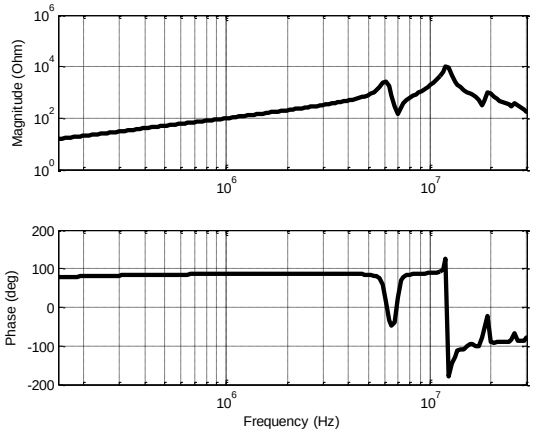

Figure 16. Impedance measurement associated with C_{m4}.

Capacitance C_{m5} given by:

$$C_{m5} = C_3' + C_4' + C_5' \quad (11)$$

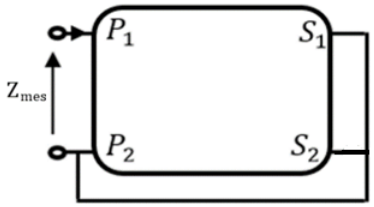

Figure 17. Configuration of the impedance C_{m5} measurement.

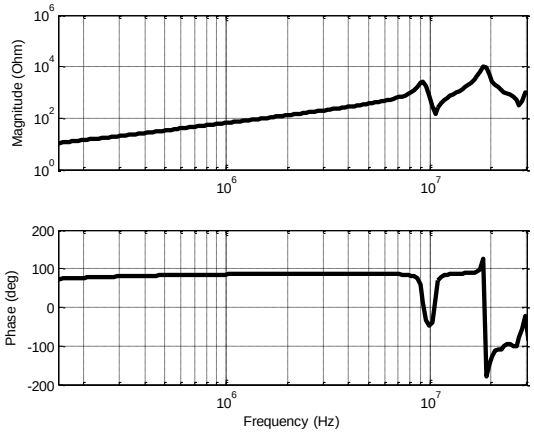

Figure 18. Impedance measurement associated with C_{m5}.

Capacitance C_{m6} given by:

$$C_{m6} = C_1' + C_2' + (\eta - 1)^2 C_3' + \eta^2 (C_4' + C_5') \quad (12)$$

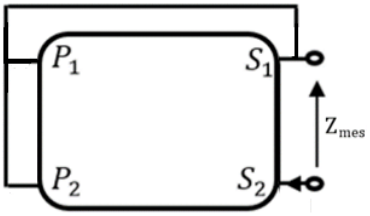

Figure 19. Configuration of the impedance C_{m6} measurement.

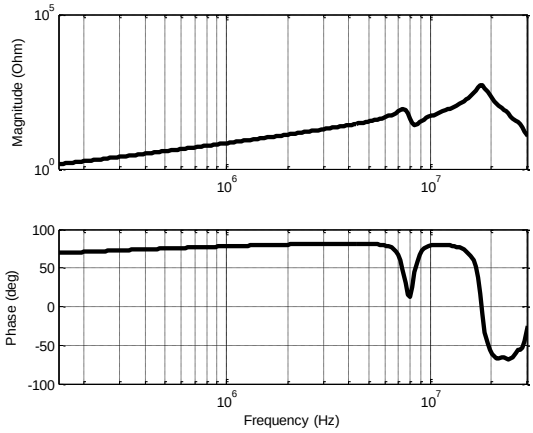

Figure 20. Impedance measurement associated with C_{m6}.

4 Model and Calculation Validation

A mathematical model can be obtained either theoretically based on physical laws or experimentally based on system measurements [33]. The measurements used to identify purpose of the model are compared.

To verify the accuracy of the used measurement technique, the overall stray capacitances are determined starting from an experimental measurement and a high-frequency equivalent circuit.

By grouping the above equations, the following expressions are obtained:

$$C_1' = C_1 \quad (13)$$

$$C_2' = C_3 + C_3' \quad (14)$$

$$C_3' = \frac{1}{2}(C_{m0} + C_{m5} - C_{m4}) + \frac{1}{\eta^2}(C_{m2} + C_{m6}) \quad (15)$$

$$C_4' = \frac{1}{2}(C_{m4} + C_{m5} - C_{m0}) \quad (16)$$

$$C_5' = \frac{1}{2}(C_{m0} + C_{m5} - C_{m4}) - C_3' \quad (17)$$

$$C_6' = C_2 + C_5' \quad (18)$$

The capacitance values are obtained from Tables 1 and 2.

Table 1. Parameters related to the capacitance measurements.

f_{r1} = 2.538 MHz	f_{r2} = 15.69 MHz	f_{r3} = 3.056 MHz
C_{m1} = 44.51 pF	C_{m2} = 1.16 pF	C_{m3} = 30.7 pF
f_{r4} = 6.082 MHz	f_{r5} = 9.283 MHz	f_{r6} = 7.368 MHz
C_{m4} = 7.75 pF	C_{m5} = 3.33 pF	C_{m6} = 5.28 pF

Table 2. Parameters related to the equivalent-circuit capacitances.

C_1= 20.01 pF	C_2 = 24.51 pF	C_3 = 18.85 pF
C_1' = 20.01 pF	C_2' = 165.59 pF	C_3' = 184.43 pF
C_4' = -144.56 pF	C_5' = -36.54 pF	C_6' = -12.04 pF

Figs. 21–26 show the differently calculated and measured impedance configurations ($C_{m1—6}$). This model is relatively in line with the impedance measurements used in our investigation. A good agreement between the calculated and measured values is shown.

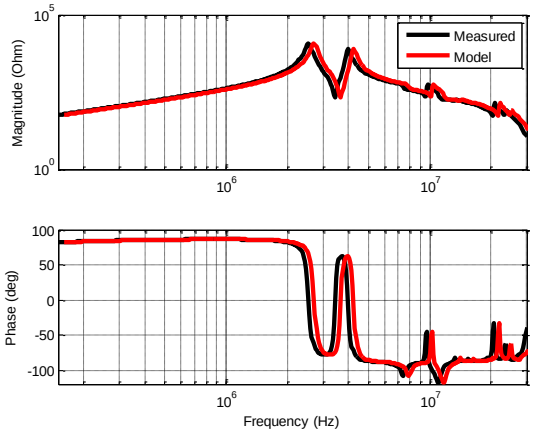

Figure 21. Measured and simulated impedance C_{m1}.

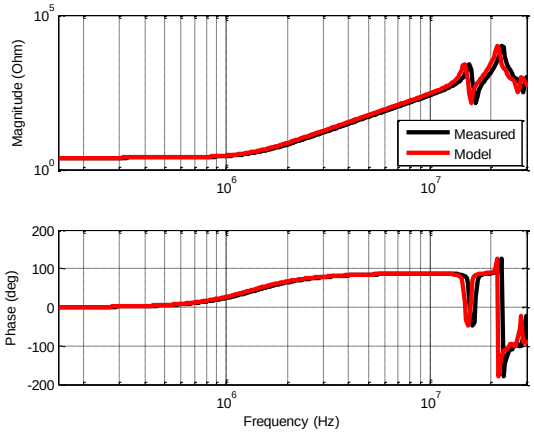

Figure 22. Measured and simulated impedance C_{m2}.

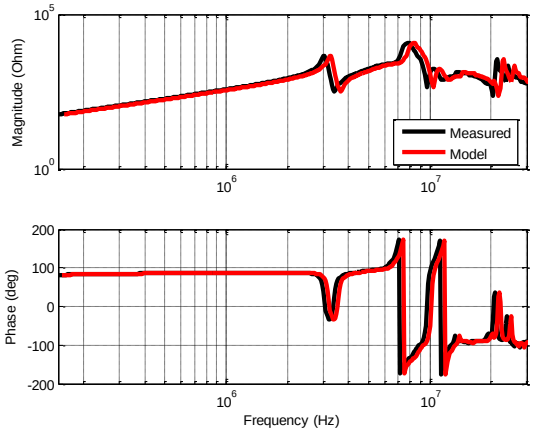

Figure 23. Measured and simulated impedance C_{m3}.

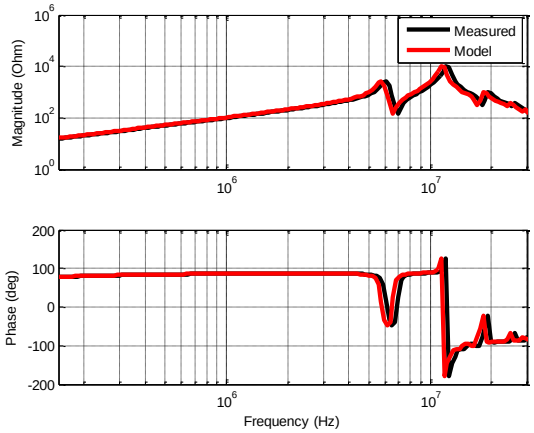

Figure 24. Measured and simulated impedance C_{m4}.

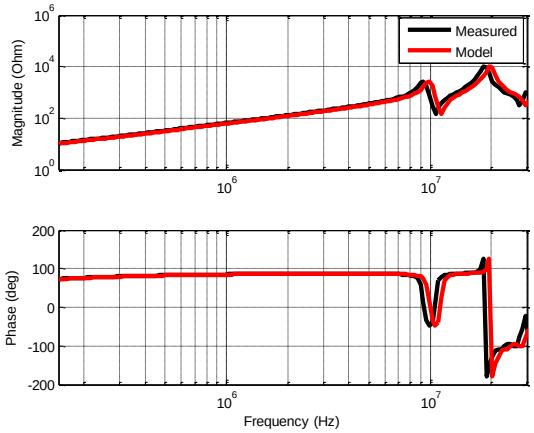

Figure 25. Measured and simulated impedance C_{m5}.

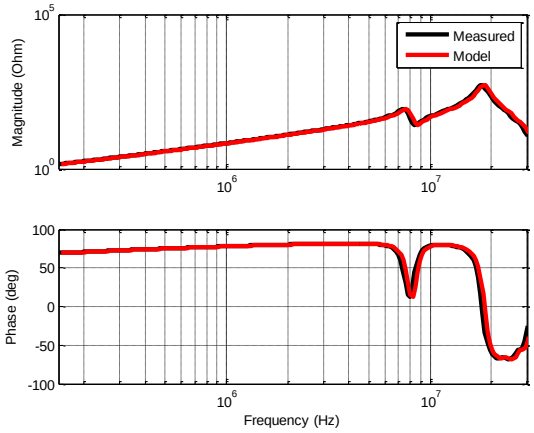

Figure 26. Measured and simulated impedance C_{m6}.

The validity of our model is tested. To compare the impedances, experimental curves and curves obtained in our model, the simulation and experimental results for different configurations are compared.

An agreement between the two systems for the high-frequency range and a convergence with the increase in the frequency value are observed. Finally, the model is found accurate for each measured impedance. The results show a good correct agreement between the studied impedances.

5 Conclusion

An experimental characterization technique and a model of a high-frequency isolating transformer are proposed. Impedance measurements and simulations for different cases are analyzed. Because of the importance of determination of parasitic capacitances in the double-winding high-frequency isolating transformer, several modeling methods and experimental investigations have been performed. A comprehensive configuration method to calculate the capacitances of the high-frequency isolating transformer is presented. Our analytical approach shows a good tradeoff between the speed of acquiring the simulation results and their accuracy. The proposed calculation method is based on a physical approach and calculation of the capacitance equations.

In practical work, the accuracy of a part of the complete circuit is often sufficient. Determining the complete circuit using the complementary measurements does not affect the lowest resonance frequencies.

References

[1] Khiem Nguyen-Duy, Ziwei Ouyang, Arnold Knott, and Michael A.E. Andersen “Minimization of the transformer inter-winding parasitic capacitance for modular stacking power supply applications”, *Proceeding of the 16th European conference on Power Electronics and Applications*, 2014.

[2] Juergen Biela and Johann W. Kolar “Using transformer parasitics for resonant converters—a review of the calculation of the stray capacitance of transformers” , *IEEE Transactions on Industry Applications*, Vol. 44, No. 1, pp. 223 - 233, 2008.

[3] I.A. Maio, F.C. Canavero, R. Franchino, D. Leonard, P. Savi “Experimental characterization and modeling of high-frequency transformers for SMPS”, *IEE International Symposium on Embedded EMC conference, Rouen, France*, 2007.

[4] F. Adam, E. Labouré, B. Révol, C. Gautier “Modélisation CEM d’un convertisseur électronique d’énergie hautes performances multi-cellulaires entrelacé couplé par transformateurs intercellules”, *15ème colloque international et exposition sur la CEM*, Limoges, 7-9 April 2010.

[5] Luca Dalessandro, Fabiana da Silveira Cavalcante, Johann W. Kolar “Self-Capacitance of High-voltage transformers”, *IEEE Transactions on Power Electronics*, Vol. 22, No. 5, pp. 2081-2092, 2007.

[6] Mohamed Miloudi, Abdelber Bendaoud, Houcine Miloudi “Common and differential modes of conducted electromagnetic interference in switching power converters”, *Rev. Roum. Sci. Techn.– Électrotechn. et Énerg.* Bucarest, Vol. 62, 3, pp. 246–251, 2017.

[7] Venkatesh Avula, Ata Zadehgol “A novel method for equivalent circuit synthesis from frequency response of multi-port networks”, *Proc. of the 2016 International Symposium on Electromagnetic Compatibility - EMC Europe*, Wroclaw, Poland, pp. 79 – 84, September 5 – 9, 2016.

[8] R. Neumayer, A. Stelzer, F. Haslinger, and R. Weigel “On the synthesis of equivalent-circuit models for multiports characterized by frequency dependent parameters”, *IEEE Transactions on Microwave Theory and Techniques*, Vol. 50, pp. 2789–2796, December 2002.

[9] Yury Kuznetsov, Andrey Baev, Anastasia Gorbunova, Maxim Konovalyuk, David Thomas,Christopher Smartt “Localization of the equivalent sources on the PCB surface by using ultra-wideband time domain near-field measurements”, *Proc. of the International Symposium on Electromagnetic Compatibility EMC Europe 2016*, Wroclaw, Poland, pp. 1–6, September 5–9, 2016.

[10] T. Filchev, A. Watson, J. Clare, P. Wheeler and F. Carastro "High voltage high frequency power transformer for pulsed power applications", *Journal of Energy and Power Engineering*, vol. 5, pp. 960 - 965, October 2010.

[11] P. Kotsampopoulos, A. Rigas "EMC issues in the interaction between smart meters and power-electronic interfaces", *IEEE Trans. Power Del*., vol. 32, no. 2, pp. 822-831, April 2017.

[12] Roman Barlik, Piotr Grzejszczak, Mariusz Zdanowski "Determination of the basic parameters of the high-frequency planar transformer", *PRZEGLĄD ELEKTROTECHNICZNY*, R. 92 NR, pp. 71-78, 6/2016.

[13] X. Margueron, J. P. Keradec "Design of equivalent circuits and characterization strategy for n-input coupled inductors", *IEEE Transactions on Industry Applications*, vol. 43, no. 1, pp. 14-22, Jan.-Feb. 2007.

[14] X. Margueron, J. P. Keradec "Identifying the magnetic part of the equivalent circuit of n-winding transformer", *IEEE Transactions on Instrumentation and Measurements*, vol. 56, no. 1, pp. 146-152, March 2006.

[15] B. Ackermann, A. Lewalter, and E. Waffenschmidt "Analytical modelling of winding capacitances and dielectric losses for planar transformers", *Proc. Comput. Power Electron. Workshop*, vol. 1, pp. 2–9, 2004.

[16] H. Y. Lu, J. G. Zhu, and S. Y. R. Hui "Experimental determination of stray capacitances in high-frequency transformers", *IEEE Trans. Power Electron*., vol. 18, no. 5, pp. 1105–1112, Aug. 2002.

[17] L. Dalessandro, F. Cavalcante, and J. W. Kolar "Calculation of the stray capacitance of high-voltage transformers", *ETH Zurich*, Zurich, Switzerland, Int. Rep. 03/04, Mar. 2004.

[18] C.Schuster and W.Fichtner "Parasitic modes on printed circuit boards and their effects on EMC and signal integrity", *IEEE Transactions on Electromagnetic Compatibility*, Vol. 45, no. 4, pp. 416 - 425, November 2003.

[19] M H Baharuddin, H Nasser, C Smartt, D W P Thomas, G Gradoni, S C Creagh, G Tanner "Measurement and wigner function analysis of field-field correlation for complex PCBs in near field", *Proc. of the International Symposium on Electromagnetic Compatibility - EMC Europe*, Wroclaw, Poland, pp. 7 – 11, September 5 – 9, 2016.

[20] N. Kuwabara, T. Nakanishi, K. Osabe, H. Muramatsu "Analysis of termination impedance influence to radiate emission from AC cable with CMAD", *Proc. Of the International Symposium on Electromagnetic Compatibility - EMC Europe*, Gothenburg, Sweden, pp. 807-812, September 1-4, 2014.

[21] Tanathep Maneenopphon, Vuttipon Tarateeraseth, Werachet Khan-ngern "The comparison of EMI and electrical performances of high frequency transformer windings for SMPS applications", *Proceeding of the Power Conversion Conference*, Nagoya, 2007.

[22] Zahir Belkaid, Philippe Enrici, François Forest, Thierry Martiré "Development of models and tool for the design of HF magnetic components in power electronics", *International Conference on Industrial Technology (ICIT)*, Lyon, France, 20-22 Feb. 2018.

[23] Dominik Grybos, Jacek Leszczynski, Cezary Swieboda, Marcin Kwiecien "Magnetic properties of composite cores made of nanocrystalline material for high frequency inductors and transformers", *Innovative Materials and Technologies in Electrical Engineering*, Sulecin, Poland, 18-20 April 2018.

[24] Keiji Tsukada, Yatsuse Majima, Yoshihiro Nakamura, Takuya Yasugi, Nannan Song "Detection of inner cracks in thick steel plates using unsaturated ac magnetic flux leakage testing with a magnetic resistance gradiometer", *IEEE Transactions on Magnetics*, Volume: 53, Issue: 11, Nov. 2017.

[25] Yi Yan, Khai D. T. Ngo, Yuhui Mei, Guo-Quan Lu "Additive manufacturing of magnetic components for power electronics integration", *International Conference on Electronics Packaging (ICEP)*, Sapporo, Japan, 20-22 April 2016.

[26] Hiroyuki Nakamoto, Daisuke Nishikubo, Shuhei Okada, Futoshi Kobayashi, Fumio Kojima "Food texture classification using magnetic sensor and principal component analysis", *Third International Conference on Computing Measurement Control and Sensor Network (CMCSN)*, Matsue, Japan, 20-22 May 2016.

[27] Jun Imaoka, Kenkichiro Okamoto, Shota Kimura "A magnetic design method considering DC-biased magnetization for integrated magnetic components used in multiphase boost converters", *IEEE Transactions on Power Electronics*, Volume: 33, Issue: 4, p.p 3346 – 3362, April 2018.

[28] A. Elrayyah, K. MPK Namburi, Y. Sozer and I. Hu- sain "An effective dithering method for electro- magnetic interference (EMI) reduction in single- phase DC/AC inverters", *IEEE Trans. Power Electron*, vol. 29, no. 6, pp. 2798-2806, June 2014.

[29] Davari, P., Hoene, E., Zare, F., & Blaabjerg, F "Improving 9-150 kHz EMI performance of single-phase PFC rectifier", *CIPS 2018 - 10th International Conference on Integrated Power Electronics Systems*, Stuttgart, Germany, pp. 1-6, March 20–22, 2018.

[30] Mario Monti, Elena Puri, Massimo Monti "Hidden aspects in CISPR 16-1-1 full compliant fast Fourier transform EMI receivers", *Proc. of the International Symposium on Electromagnetic Compatibility - EMC Europe*, Wroclaw, Poland, pp. 34 – 39, September 5 – 9, 2016.

[31] Anders P. Mynster & Per Thåstrup Jensen "EMC for the IoT", *Proc. of the International Symposium on Electromagnetic Compatibility - EMC Europe*, Wroclaw, Poland, pp. 144 – 149, September 5 – 9, 2016.

[32] S. Braun, T. Donauer, and P. Russer "A real-time time-domain EMI measurement system for full-compliance measurements according to CISPR 16-1-1", *IEEE Trans. on Electromagnetic Compatibility*, vol. 50, no. 2, pp. 259–267, 2008.

[33] Houcine Miloudi, Abdelber Bendaoud, Mohamed Miloudi "A method for modeling a common-mode impedance for the AC motor", Rev. *Elektrotehniški Vestnik*, 84(5):pp.241-246, 2017.

Mohamed Miloudi received his Ph.D. degree in Electrical Engineering from the Faculty of Electrical Engineering of the UDL University in 2018. He is currently a Lecturer at the Electrical Engineering department of the Ahmed Zabana University Center. His research interests include electromagnetic compatibility, EMI reduction techniques and electronic power converters.

Houcine Miloudi received his Ph.D. degree in Electrical Engineering from the Faculty of Electrical Engineering of the UDL University in 2012. He is currently a Lecturer in the Faculty of Electrical Engineering of the UDL University. His research interests include electromagnetic compatibility (EMC) in power converter, EMI reduction techniques, high-frequency power conversion, magnetic design and power electronics.

Abdelber Bendaoud received his Ph.D. degree in Electrical Engineering from the Faculty of Electrical Engineering of the UDL University in 2004. He is currently a Professor in the Faculty of Electrical Engineering of the UDL University. His research interests include electrostatic separation technologies, high-voltage insulation, gas discharges, electric and magnetic fields, and EMC.

Mohammed Adnan Salhi received his Ph.D. degree in Physikalisch-Technische Bundesanstalt (PTB), Braunschweig, Germany in 2009. He is currently a Lecturer at the Physikalisch-Technische Bundesanstalt (PTB), the National Metrology Institute of Braunschweig. His research interests include electromagnetic compatibility (EMC), frequency and electromagnetic fields and antenna measurement techniques.

Ahmad N. Al-Omari received his Ph.D. degree from Colorado State University USA in 2006. He is currently a Professor in the Electronics Engineering Department, Hijjawi Faculty for Engineering Technology, Yarmouk University. His research interests include design, fabrication, characterization and modeling of high-speed oxide-confined vertical-cavity surface-emitting lasers (VCSELs) and dielectrics for high-speed devices.